FRACTIONAL-ORDER DIFFUSION FOR IMAGE RECONSTRUCTION

Stanislas Larnier

Institut de Mathématiques de Toulouse
Université Paul Sabatier, Toulouse, France
slarnier@math.univ-toulouse.fr

Roberto Mecca

Dipartimento di Matematica "G. Castelnuovo"
Sapienza - Universitá di Roma, Roma, Italia
roberto.mecca@mat.uniroma1.it

ABSTRACT

In this paper, a general framework based on fractional-order partial differential equations allows to solve image reconstruction problems. The algorithm presented in this work combines two previous notions: the fractional derivative implementation [1] and the edge detection by topological gradient [2]. The purpose of the paper is to extend some existing results in image denoising problem with fractional-order diffusion equations and presents new results in image inpainting. The results emphasize the importance of particular fractional-orders.

Index Terms— Fractional-order partial differential equation, topological gradient, image denoising, image inpainting.

1. INTRODUCTION

Our purpose is to minimize the following functional:

$$\mathcal{F}_\alpha(u) = \|c^{\frac{1}{2}}\nabla^\alpha u\|^2_{L^2(\Omega)} + \|Lu - v\|^2_E \qquad (1)$$

where α represents the order of the derivative with a finite L^2 norm (i.e minimization in the $H^{2\alpha} \equiv W^{2\alpha,2}$ space functions with $\alpha > 0$), L is a linear observation operator and the space E corresponds to $L^2(\Omega)$ in the restoration case and $L^2(\Omega\backslash\omega)$ in the inpainting case with $\omega \subset \Omega$ is an unkwown subset.

The main idea of this paper is to use fractional derivatives for the regularization term instead of integer derivatives. In the last 30 years, fractional calculus began to shift from pure mathematics formulations to applications in various fields including biology, physics and mechanics. In particular in the image processing field [1, 3, 4], the nonlocal properties of fractional differential-based approaches appear to give better results than traditional integral-based algorithms.

The minimization of the functional (1) is equivalent to consider the associated Euler-Lagrange equation:

$$\begin{cases} -\nabla^\alpha \cdot (c\nabla^\alpha u) + L^*Lu = L^*v & \text{in } \Omega, \\ \nabla^\alpha u \cdot n = 0 & \text{on } \partial\Omega. \end{cases} \qquad (2)$$

where n is the external normal to the boundary $\partial\Omega$ and L^* the adjoint operator of L.

In [1], Bai and Feng use fractional derivatives for image denoising with an iterative process. However, the computing time remains a major drawback of their method and the first contribution of this paper proposes an efficient algorithm able to solve this issue. Whereas in [1], the diffusion coefficient $c(\mathbf{x})$, which depends on the space variable, evolves during the iterative process, we propose to fix it and reconstruct the image in one iteration using the topological gradient information [2, 5, 6]. The second contribution is related to the fact that the algorithm is also able to solve inpainting problems.

Section 2 recalls a way to calculate fractional derivative using Fourier transform. Section 3 is dedicated to edge detection by topological gradient method. In Section 4, our image reconstruction algorithm is presented. Section 5 compares the numerical results in image denoising with the Bai and Feng's algorithm, and some denoising and inpainting applications are performed and compared with other established methods involving partial differential equations.

2. FRACTIONAL DERIVATIVES

This section recalls the implementation of the fractional order gradient from Bai and Feng [1]. For the next, let $D^\alpha \equiv \nabla^\alpha$ be the fractional operator having the same structure as the gradient operator, that is $D^\alpha u = \nabla^\alpha u = (D_x^\alpha u, D_y^\alpha u)$. The computation of fractional derivative is given for the discrete image domain where it is assumed that u has $m \times m$ pixels. This domain consists of uniformly spaced points starting at $(0,0)$, with $u(x,y) = u(x\Delta x, y\Delta y)$ for $x, y = 0, \ldots, m-1$, where the grid size is chosen so that $\Delta x = \Delta y = 1$. The following definition of two-dimensional Discrete Fourier Transform (2D-DFT) is used

$$F(u)(w_1, w_2) = \frac{1}{m^2}\sum_{x,y=0}^{m-1} u(x,y)\exp\left(-i2\pi\frac{w_1 x + w_2 y}{m}\right).$$

Using the gradient approximation with the finite difference, it is possible to write the relation $F(u - T_x u) = K_x^1 F(u)$ where $K_x^1 = \text{diag}\left(1 - \exp\left(-i2\pi\frac{w_1}{m}\right)\right)$ is a diagonal operator and T_x a translation operator with periodic boundary conditions, $T_x u(x,y) = u(x-1, y)$. We have

$$D_x^\alpha u = F^{-1}\left(K_x^\alpha F(u)\right), \qquad (3)$$

where $K_x^\alpha = \text{diag}\left(\left(1 - \exp\left(-i2\pi\frac{w_1}{m}\right)\right)^\alpha\right)$.

In order to use a centred difference scheme to compute the fractional derivative, a translation of D_x^α is made by $\frac{\alpha}{2}$. The fractional derivative takes the following form

$$\tilde{D}_x^\alpha u = D_x^\alpha\left(\mathfrak{u}\left(x + \frac{\alpha}{2}, y\right)\right), \tag{4}$$

where $\mathfrak{u}$ is the interpolation of u outside the discrete set of points of the image. As a correspondence of this equivalence (4) it is possible to write the following relation:

$$\tilde{D}_x^\alpha u = F^{-1}\left(\tilde{K}_x^\alpha F(u)\right), \tag{5}$$

where $\tilde{K}_x^\alpha = \text{diag}\left(\left(1 - \exp\left(-i2\pi\frac{w_1}{m}\right)\right)^\alpha \exp\left(i\pi\alpha\frac{w_1}{m}\right)\right)$.

The adjoint operator $\tilde{D}_x^{\alpha*}$ is defined as follows:

$$\tilde{D}_x^{\alpha*} u = F^{-1}\left(\tilde{K}_x^{\alpha*} F(u)\right). \tag{6}$$

3. TOPOLOGICAL GRADIENT

The information about the edges is determined with $\alpha = 1$. The minimization of $\mathcal{F}_1(u)$, Equation (1), is equivalent to the problem of finding $u \in H^1(\Omega)$ such that

$$\begin{cases} -\nabla \cdot (c\nabla u) + L^*Lu = L^*v & \text{in } \Omega, \\ \partial_n u = 0 & \text{on } \partial\Omega, \end{cases} \tag{7}$$

where ∂_n denotes the normal derivative to $\partial\Omega$.

At a given point $\mathbf{x}_0 \in \Omega$, a small isolated crack σ_ρ is inserted and $\sigma_\rho = \mathbf{x}_0 + \rho\sigma(n)$ where $\sigma(n)$ is a straight crack, n is a unit vector normal to the crack and $\rho > 0$ is the length of the crack. Let $\Omega_\rho = \Omega\backslash\sigma_\rho$ be the perturbed domain. The perturbed solution $u_\rho \in H^1(\Omega_\rho)$ satisfies

$$\begin{cases} -\nabla \cdot (c\nabla u_\rho) + L^*Lu_\rho = L^*v & \text{in } \Omega, \\ \partial_n u_\rho = 0 & \text{on } \partial\Omega, \\ \partial_n u_\rho = 0 & \text{on } \sigma_\rho. \end{cases} \tag{8}$$

The edge detection method consists in looking for a crack σ such that the energy $j(\rho) = J_\rho(u_\rho) = \frac{1}{2}\int_{\Omega_\rho} |\nabla u_\rho|^2$ is as small as possible, see [2]. This amounts to saying that the energy outside the edges is as small as possible.

The cost function j has the following asymptotic expansion

$$j(\rho) - j(0) = \rho^2 g(\mathbf{x}_0, n) + o(\rho^2), \tag{9}$$

where the topological gradient g is given by

$$g(\mathbf{x}_0, n) = -\pi(\nabla u_0(\mathbf{x}_0) \cdot n)(\nabla p_0(\mathbf{x}_0) \cdot n) - \pi|\nabla u_0(\mathbf{x}_0) \cdot n|^2. \tag{10}$$

The solution of the adjoint problem

$$\begin{cases} -\nabla \cdot (c\nabla p_0) + L^*Lp_0 = -\partial_u J_0(u_0) & \text{in } \Omega, \\ \partial_n p_0 = 0 & \text{on } \partial\Omega, \end{cases} \tag{11}$$

is p_0 that, together with u_0, is calculated in the initial domain without cracks. The edges are located at points where the topological gradient is the most negative.

4. ALGORITHM

In order to reduce the discontinuities across the image border due to the periodization, the image is reflected symmetrically across the border in the same way as [1].

The aim is to solve the following equation:

$$\tilde{D}_x^{\alpha*} c_x \tilde{D}_x^\alpha u + \tilde{D}_y^{\alpha*} c_y \tilde{D}_y^\alpha u + u = v \tag{12}$$

In order to obtain a diffusion function in the vertical and horizontal directions, the definition of the topological gradient g (10) can be simplified as:

$$\begin{aligned} g_x(\mathbf{x}) &= -\pi c\partial_1 u_0(\mathbf{x})\partial_1 p_0(\mathbf{x}) - \pi(\partial_1 u_0(\mathbf{x}))^2, \\ g_y(\mathbf{x}) &= -\pi c\partial_2 u_0(\mathbf{x})\partial_2 p_0(\mathbf{x}) - \pi(\partial_2 u_0(\mathbf{x}))^2. \end{aligned} \tag{13}$$

Algorithm 1 solve the image reconstruction problem (1)

Input: v, c_0, ϵ and δ. **Output:** u

1: Initialization: $c_i = c_0$, i is x or y.
2: Compute u_0 and p_0, solutions of the direct (7) and adjoint (11) problems.
3: Compute g_x and g_y given by Equations (13).
4: Set $c_i(\mathbf{x}) = \begin{cases} \epsilon & \text{if } g_i(\mathbf{x}) < \delta, \\ c_0 \exp\left((g_i(\mathbf{x}) - \delta)/|\delta|\right) & \text{otherwise.} \end{cases}$
5: Using the Fourier transform and the centred scheme, solve the equation $\tilde{D}_x^{\alpha*} c_x \tilde{D}_x^\alpha u + \tilde{D}_y^{\alpha*} c_y \tilde{D}_y^\alpha u + u = v$.

The algorithms were coded in MATLAB. The reconstructions are compared using Peak Signal to Noise Ratio (PSNR) expressed in dB and the Structural SIMilarity (SSIM) [7].

5. NUMERICAL RESULTS

Table 1 provides a comparison between Bai and Feng algorithm [1] and Algorithm 1, the images are corrupted by an additive Gaussian noise of standard deviation σ. When $\sigma = 15$, the diffusion coefficient c_0 and the threshold δ are $c_0 = 1.3$, $\delta = -300$ for the Lena and Peppers images and $c_0 = 1$, $\delta = -300$ for the Boat image. When $\sigma = 25$, the diffusion coefficient c_0 and the threshold δ are $c_0 = 2$, $\delta = -300$ for the Boat and Peppers images and $c_0 = 2.5$, $\delta = -400$ for the Lena image. The same diffusion coefficient c_0 and the threshold δ are applied to all α to emphasize the fractional order influence. One can remark that for each image, the PSNR and SSIM values have one peak located most generally near 1.5 and 1.75. Figure 1 shows the reconstructions obtained with $\sigma = 15$ and $\alpha = 1.5$.

Table 2 compares the CPU relative to restoration processes for $\alpha = 1$ and 1.5 carried out for Bai and Feng's algorithm [1] and for Algorithm 1. The tests have been made on the same computer with MATLAB. Our algorithm needs a shorter computing time to achieve similar quality results.

A comparison is made in Table 3 with the results of Algorithm 1 with $\alpha = 1.5$ and two denoising algorithms. The first

	α	1		1.25		1.5		1.75		2	
Images	Method	PNSR	SSIM	PNSR	SSIM	PNSR	SSIM	PNSR	SSIM	PNSR	SSIM
Lena	BF [1]	31.58	843	32.57	865	32.77	870	**32.81**	**870**	32.26	855
$\sigma = 15$	Algo 1	32.38	845	32.58	853	32.55	858	32.29	856	32.18	854
Lena	BF [1]	29.19	791	30.26	822	30.49	**830**	**30.50**	**830**	29.74	797
$\sigma = 25$	Algo 1	30.19	801	30.29	807	30.26	809	30.11	807	30.02	803
Boat	BF [1]	29.82	792	30.53	811	30.63	814	30.61	813	30.07	795
$\sigma = 15$	Algo 1	30.43	803	30.73	815	**30.76**	**820**	30.32	812	30.06	806
Boat	BF [1]	27.35	712	28.11	738	28.22	743	28.12	740	27.54	705
$\sigma = 25$	Algo 1	28.17	732	28.38	744	**28.44**	**749**	28.18	744	28.01	739
Peppers	BF [1]	30.81	873	31.95	901	32.11	906	32.27	**909**	31.52	892
$\sigma = 15$	Algo 1	31.97	885	32.33	897	**32.38**	903	32.07	905	31.92	903
Peppers	BF [1]	27.94	812	29.12	851	29.35	861	29.46	**864**	28.59	828
$\sigma = 25$	Algo 1	28.78	793	29.28	818	**29.56**	841	29.32	845	29.17	842

Table 1. Image denoising with Bai and Feng algorithm [1] and with Algorithm 1.

Fig. 1. From left to right, the noisy image with $\sigma = 15$, the reconstructions with respectively Bai and Feng's algorithm [1] and Algorithm 1, the fractional order α is equal to 1.5. From top to bottom, the Lena, Boat and Peppers images.

Boat	$BF_{\alpha=1}$	$Algo_{\alpha=1}$	$BF_{\alpha=1.5}$	$Algo_{\alpha=1.5}$
PSNR	27.35	28.17	28.22	28.44
SSIM	712	732	743	794
CPU (s)	940	45	1820	70

Table 2. CPU for Bai and Feng's algorithm [1] and for our algorithm with $\alpha = 1$ and 1.5 applied on the noisy Boat image with $\sigma = 25$.

		Lena	Boat	Peppers
Method	σ	PSNR / SSIM	PSNR / SSIM	PSNR / SSIM
Algo 1	15	**32.55 / 858**	**30.76 / 820**	**32.38 / 903**
$\alpha = 1.5$	25	**30.26 / 809**	**28.44 / 794**	**29.53 / 839**
ROF	15	31.61 / 841	30.42 / 810	31.48 / 881
[8]	25	28.99 / 754	27.91 / 725	28.59 / 800
Weickert	15	29.82 / 714	29.22 / 735	29.84 / 759
[9]	25	26.00 / 535	25.69 / 573	25.91 / 592

Table 3. Comparison of different denoising algorithms.

one, the Rudin-Osher-Fatemi algorithm solves the problem using a method based on total variation [8]. The second one uses an algorithm proposed by Weickert [9]. One can note that the best quality in PSNR and SSIM are obtained with the fractional derivative denoising algorithm. Figure 2 presents the results of the Boat image.

	Lena	Boat	Peppers
Method	PSNR / SSIM	PSNR / SSIM	PSNR / SSIM
$Algo_{\alpha=1.5}$	**30.12 / 863**	**26.84 / 767**	**27.84 / 888**
Laplacian	28.31 / 854	26.46 / **771**	26.48 / 868
TV [10]	27.48 / 830	25.35 / 735	25.81 / 851

Table 4. Comparison of different inpainting algorithms with 80% unknown pixels.

A comparative study of inpainting reconstruction methods has been performed. In this experiment, the diffusion coefficient c_0 and the threshold δ are respectively equal to 0.1 and -500. Table 4 presents the results of different numerical schemes. The first one uses the approximation of a Laplace equation with homogeneous boundary conditions. The second one is based on total variation minimization; it uses the split Bregman method improved by Goldstein and Osher [10]. Figure 3 presents the results on the Lena image from Table 4.
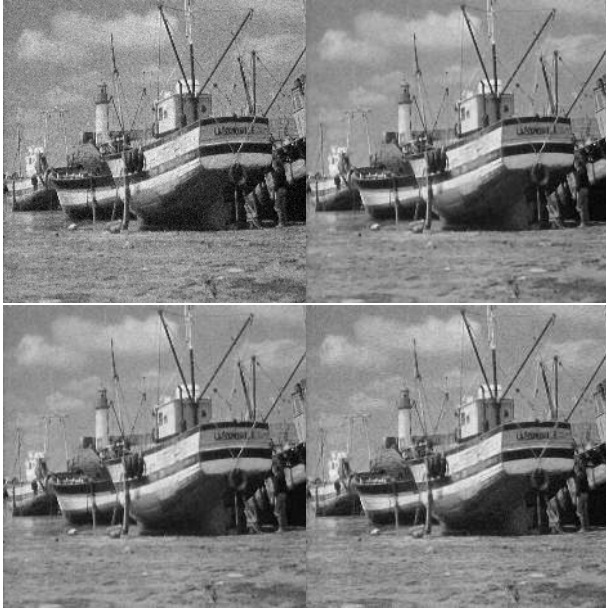
Fig. 2. From left to right and up to down, the noisy Boat image, the reconstruction with respectively Algorithm 1, Rudin-Osher-Fatemi's algorithm [8] and Weickert's algorithm [9].

Fig. 3. From left to right and up to down, the reconstruction with respectively Algorithm 1, Laplace equation and total variation regularization [10].

6. CONCLUSION

This work proposes new applications of fractional-order partial differential equations in image processing. Our studies led to proposing a general reconstruction algorithm that incorporates the fractional derivative implementation from [1] and the edge detection by topological gradient from [2]. Concerning denoising, better results are obtained with an order α which is fractional rather than integer. The interesting values for the fractional order α seem to be around 1.5 and 1.75. It corroborates previous results [1]. Contrary to existing iterative processes with a fractional order, the algorithm presented here is non iterative. It gives similar results for a shorter computer time and can be used to solve inpainting problems. The comparison with state-of-the-art methods involving partial differential equations showed better results in terms of quality.

7. REFERENCES

[1] J. Bai and X.-C. Feng, "Fractional-order anisotropic diffusion for image denoising," *IEEE transactions on image processing*, vol. 16, no. 10, pp. 2492–2502, 2007.

[2] L. J. Belaid, M. Jaoua, M. Masmoudi, and L. Siala, "Image restoration and edge detection by topological asymptotic expansion," *C. R. Acad. Sci. Paris*, vol. 342, no. 5, pp. 313–318, March 2006.

[3] E. Cuesta and J.F. Codes, "Image processing by means of a linear integro-differential equation," in *3rd IASTED Int. Conf. Visualization, Imaging and Image Processing*, 2003, vol. 1, pp. 438–442.

[4] S. Didasa, B. Burgeth, A. Imiya, and J. Weickert, "Regularity and scalespace properties of fractional high order linear filtering," *Scale Spaces and PDE Methods in Computer Vision*, pp. 13–25, 2005.

[5] D. Auroux and M. Masmoudi, "Image processing by topological asymptotic expansion," *J. Math. Imaging Vision*, vol. 33, no. 2, pp. 122–134, February 2009.

[6] S. Larnier and J. Fehrenbach, "Edge detection and image restoration with anisotropic topological gradient," in *International Conference on Acoustics Speech and Signal Processing (ICASSP)*, March 2010, pp. 1362 –1365.

[7] Z. Wang, A. C. Bovik, H. R. Sheikh, and E. P. Simoncelli, "Image quality assessment : From error visibility to structural similarity," *IEEE Transactions on Image Processing*, vol. 13, no. 4, pp. 600–612, April 2004.

[8] L. I. Rudin, S. Osher, and E. Fatemi, "Nonlinear total variation based noise removal algorithms," *Communication on Pure and Applied Mathematics*, vol. 60, no. 1, pp. 259–268, 1992.

[9] J. Weickert, *Anisotropic Diffusion in Image Processing*, Ph.d. thesis, Dept. of Mathematics, University of Kaiserslautern, Germany, 1996.

[10] T. Goldstein and S. Osher, "The split Bregman method for L1 regularized problems," *SIAM Journal on Imaging Sciences*, vol. 2, no. 2, pp. 323–343, 2009.